Electronic Supplementary Material (ESI) for Journal of Materials Chemistry A.

Electronic Supplementary information

BCN Network-Encapsulated Multiple Phases of Molybdenum Carbide for Efficient Hydrogen Evolution Reaction in Acidic and Alkaline Media

Mohsin Ali Raza Anjum, Min Hee Lee and Jae Sung Lee*

School of Energy and Chemical Engineering, Ulsan National Institute of Science and Technology (UNIST), 50 UNIST-gil, Ulsan 44919, South Korea

This file includes supplementary Figures S1-S20, and Tables S1- S6.

Table S1. Composition of starting materials for preparation of multiple phase of molybdenum carbides

Name	Imidazole	Boric acid	$MoCl_5$
o-β-Mo_2C	5 mmol	NIL	1 mmol
o-α-Mo_2C@BCN	5 mmol	1 mmol	1 mmol
h-η-MoC@BCN	5 mmol	2 mmol	1 mmol
h-β-Mo_2C@BCN	5 mmol	3 mmol	1 mmol
c-α-Mo_2C@BCN	5 mmol	4 mmol	1 mmol
o-β-Mo_2C@BCN	5 mmol	5 mmol	1 mmol

Imidazole = $(CH)_2N(NH)CH$: Boric acid = H_3BO_3

Table S2. Information of multiple phases of as synthesized molybdenum carbides

Name	Phase	Crystal system	Space group	Reference code	Crystal view
o-α-Mo_2C@BCN	α-Mo_2C like Ni_2C	Orthorhombic	Pbcn	01-071-0242	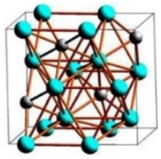 J. Phys.: Condens. Matter 2010,22, 445503
h-η-MoC@BCN	η-MoC	Hexagonal	P63/mmc	01-089-4305	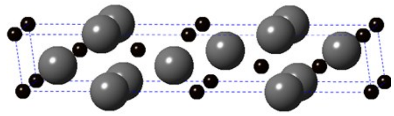 Angew. Chem, 2014, 126, 6525
h-β-Mo_2C@BCN	β-Mo_2C	Hexagonal	P63/mmc	03-065-8364	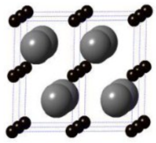 Angew. Chem, 2014, 126, 6525
c-α-MoC_{1-x}@BCN	α-MoC_{1-x} & α-Mo_2C	Cubic Orthorhombic	Fm3m	03-065-0280 01-071-0242	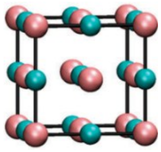 Phys. Chem. Chem. Phys., 2013, 15, 12617
o-β-Mo_2C@BCN	β-Mo_2C	Orthorhombic	Pca21	01-077-0720	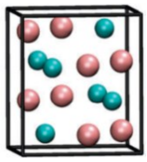 Phys. Chem. Chem. Phys., 2013, 15, 12617

Table S3. Surface composition of each phase of molybdenum carbides determined by XPS

Sample	Mo [At. %]	C [At. %]	N [At. %]	B [At. %]	O [At. %]
o-α-Mo_2C@BCN	10.44	60.81	17.37	1.04	10.34
h-η-MoC@BCN	10.39	55.93	24.27	1.23	8.18
h-β-Mo_2C@BCN	11.03	59.09	21.17	1.60	7.11
c-α-Mo_2C@BCN	11.3	60.02	18.7	3.15	6.83
o-β-Mo_2C@BCN	13.50	60.49	12.84	4.05	9.12

Table S 4. Comparison of HER performance in acid (0.5M H_2SO_4) media with other molybdenum carbides based electrocatalysts

Catalyst	Onset (mV)	η1 (mV)	η10 (mV)	Tafel Slope (mV/dec)	J_0 (mA/cm²)	Electrolyte
c-α-MoC_{1-x}@BCN	20	25	124	47 167	0.124 1.505	0.5M H_2SO_4
h-β-Mo_2C@BCN	20	30	140	103	0.392	0.5M H_2SO_4
o-β-Mo_2C@BCN	48	76	168	80	0.109	0.5M H_2SO_4
h-η-MoC@BCN	45	101	182	67	0.006	0.5M H_2SO_4
o-α-Mo_2C@BCN	40	120	195	73	0.011	0.5M H_2SO_4
Mo_2C-carbon nanocomposites[1]		160	260	110		0.5M H_2SO_4
$Mo_{0.06}W_{1.94}C$/CB[2]		150	220			0.5M H_2SO_4
Mo_2C/Graphitic Carbon Sheets[3]	120	160	210	62.6	0.0125	0.5M H_2SO_4
Mo_2C[4]		155	210	56	0.0013	0.5M H_2SO_4
Mo_2C NWs[5]	110	115	200	55.8		0.5M H_2SO_4
Mo_2C nanoparticles[6]		150	198	56		0.5M H_2SO_4
MoS_2/Mo_2C embedded N-CNT[7]	145		190	69		0.5M H_2SO_4
Mo1Soy(β-Mo_2C and γ-Mo_2N)[8]		120	177	66.4	0.037	0.1M $HClO_4$
MoS_x@Mo_2C[9]	120	130	170	52	0.131	0.5M H_2SO_4
Mo_2C on CNT[10]		63	152	55.2	0.014	0.1M $HClO_4$
Ni-Mo_2C nano-rod[11]	80	100	150	58	0.033	0.5M H_2SO_4
3D Mo_xC/Ni network[12]		44	150	49		0.5M H_2SO_4
Mo_2C–NCNT[13]	65	72	147	71	0.114	0.5M H_2SO_4
MoCN[14]	50	55	145	46		0.5M H_2SO_4
Mesoporous η-MoC_x nano-octahedrons[15]		87	142	53		0.5M H_2SO_4
Mo_2C, CNT-Graphene composite[16]	62	90	130	58	0.062	0.5M H_2SO_4
Mo_2C on RGO[17]	70	91	130	57.3		0.5M H_2SO_4
nanoporous Mo_2C nanowires[18]		70	130	53		0.5M H_2SO_4
Mo_2C@NC[19]	-	60	124	60	0.096	0.5M H_2SO_4
NS-doped Mo_2C[20]	46	56	86	47	0.038	0.5M H_2SO_4
Mo_xC-Ni@NCV[21]	20	22	75	45		0.5M H_2SO_4
β- Mo_2C[22]		205		120	0.01729	0.5M H_2SO_4

Table S5. Comparison of HER performance of multiple phases of molybdenum carbides encapsulated by BCN with other Mo_2C-based electrocatalysts in alkaline media

Catalyst	Onset (mV)	η1 (mV)	η10 (mV)	Tafel Slope (mV/dec)	J_0 (mA/cm²)	Electrolyte
***h*-β-Mo$_2$C@BCN**		45	92	52.8	0.162	1.0M NaOH
***h*-η-Mo$_2$C@BCN**		65	116	53.4	0.063	1.0M NaOH
***o*-α-Mo$_2$C@BCN**		63	119	58.5	0.0861	1.0M NaOH
***o*-β-Mo$_2$C@BCN**		69	126	60	0.075	1.0M NaOH
***c*-α-MoC$_{1-x}$@BCN**		73	141	73	0.113	1.0M NaOH
***h*-β-Mo$_2$C@BCN**		46	98	55	0.162	1.0M KOH
***h*-η-Mo$_2$C@BCN**		52	106	55.4	0.120	1.0M KOH
***o*-α-Mo$_2$C@BCN**		49	111	68	0.218	1.0M KOH
***o*-β-Mo$_2$C@BCN**		56	110	59	0.127	1.0M KOH
***c*-α-MoC$_{1-x}$@BCN**		62	154	98	0.225	1.0M KOH
Dual-doped Co@BCN[23]		70	183	73.2		1.0M KOH
Mo$_2$C–NCNT[13]	190	195	257			1.0M KOH
Mo$_2$C[24]		130	190	54	0.0038	1.0M KOH
Mo$_2$C nanoparticles[6]		110	176	58		1.0M KOH
Mesoporous η-MoC$_x$ nano-octahedrons[15]		92	151	59		1.0M KOH
Mo$_2$C nano-rod Ni impregnated Mo$_2$C nano-rod[11]		48	130	49	0.27	1.0M KOH
Mo$_2$C@NC[19]	-	10	60			1.0M KOH

Table S6. Electrochemical active surface area (ECSA) and specific capacitance of all composites

$$A_{ECSA} = \frac{Specific\ Capacitance}{40\ \mu F.cm^{-2}\ per\ cm^2_{ECSA}}$$ **Ref.** [25]

Sample	C (µF/cm²)	A_{ECSA} (cm^2_{ECSA})	C (µF/cm²)	A_{ECSA} (cm^2_{ECSA})	C (µF/cm²)	A_{ECSA} (cm^2_{ECSA})
	0.5M H_2SO_4		1.0M NaOH		1.0M KOH	
o-α-Mo$_2$C@BCN	13910	348	14090	352	17800	445
h-η-Mo$_2$C@BCN	4170	104	10340	258	6410	160
h-β-Mo$_2$C@BCN	5610	140	5910	148	4990	125
c-α-MoC$_{1-x}$@BCN	9280	232	6600	165	7090	177
o-β-Mo$_2$C@BCN	2430	61	401.82	10	1500	37.5

Please do not adjust margins

A

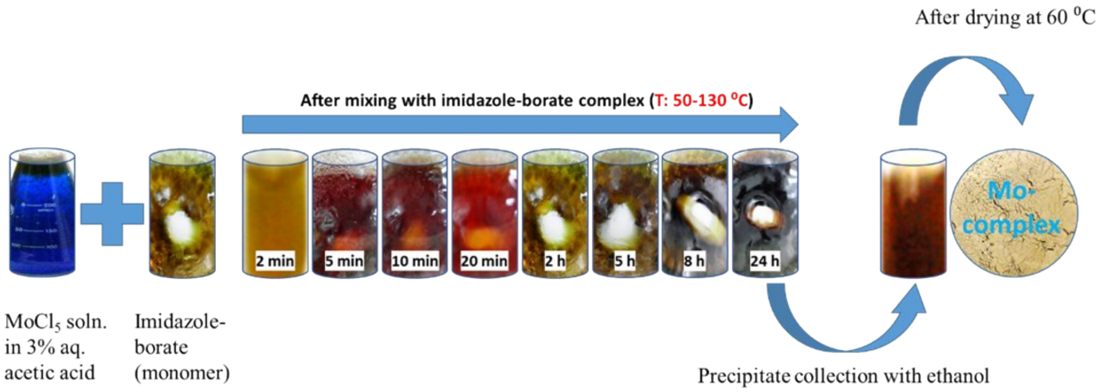

B

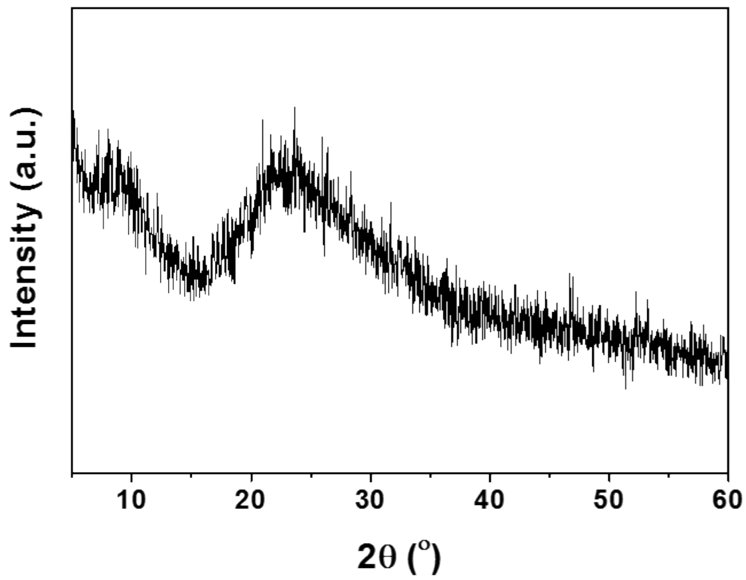

Figure S1. (A) Color change with reaction time and collected organometallic complex precipitate. (B) XRD pattern of a Mo-Im-Borate organometallic complex

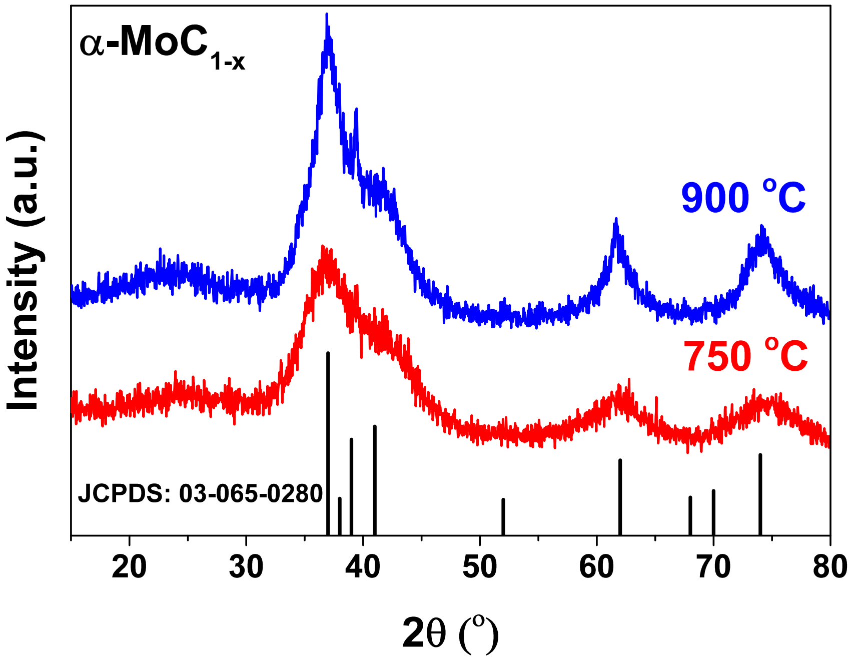

Figure S2. XRD pattern of c-α-MoC_{1-x} synthesized at 750 and 900 ^{0}C (JCPDS 03-065-0280)

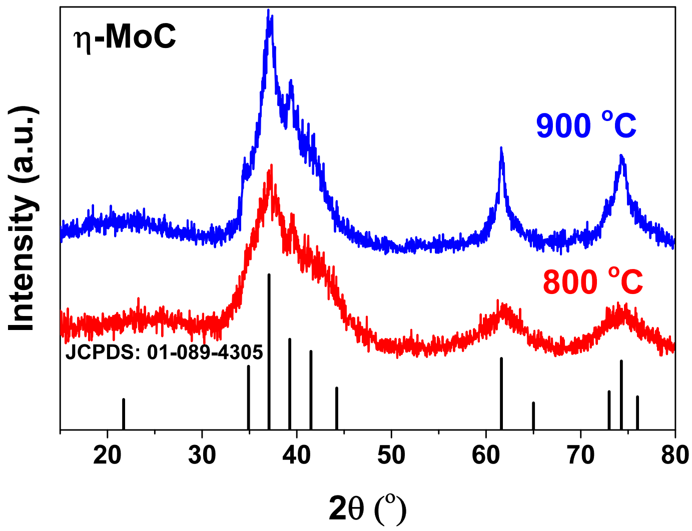

Figure S3. XRD pattern of h-η-MoC synthesized at 800 and 900 ^{0}C (JCPDS 01-089-4305)

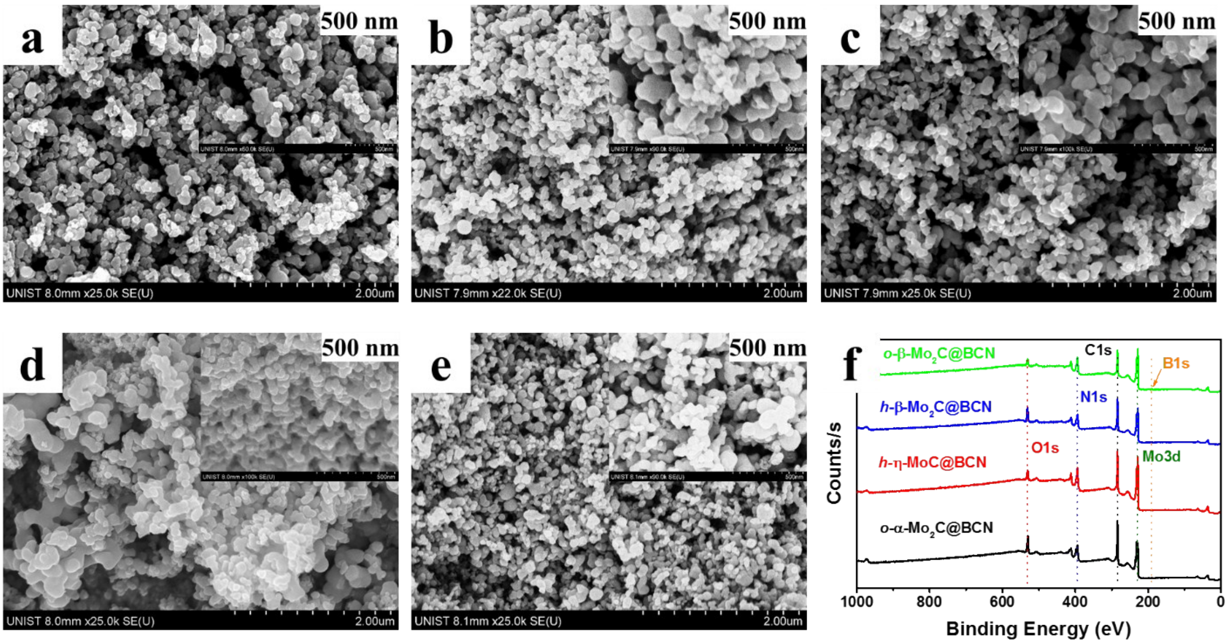

Figure S4. FESEM images and XPS survey. (**a**) Orthorhombic α-Mo_2C@BCN. (**b**) Hexagonal η-MoC@BCN. (**c**) Hexagonal β-Mo_2C@BCN. (**d**) Cubic α –MoC_{1-x}@BCN. (**e**) Orthorhombic β-Mo_2C@BCN. (**f**) XPS survey of multiple phases of molybdenum carbides

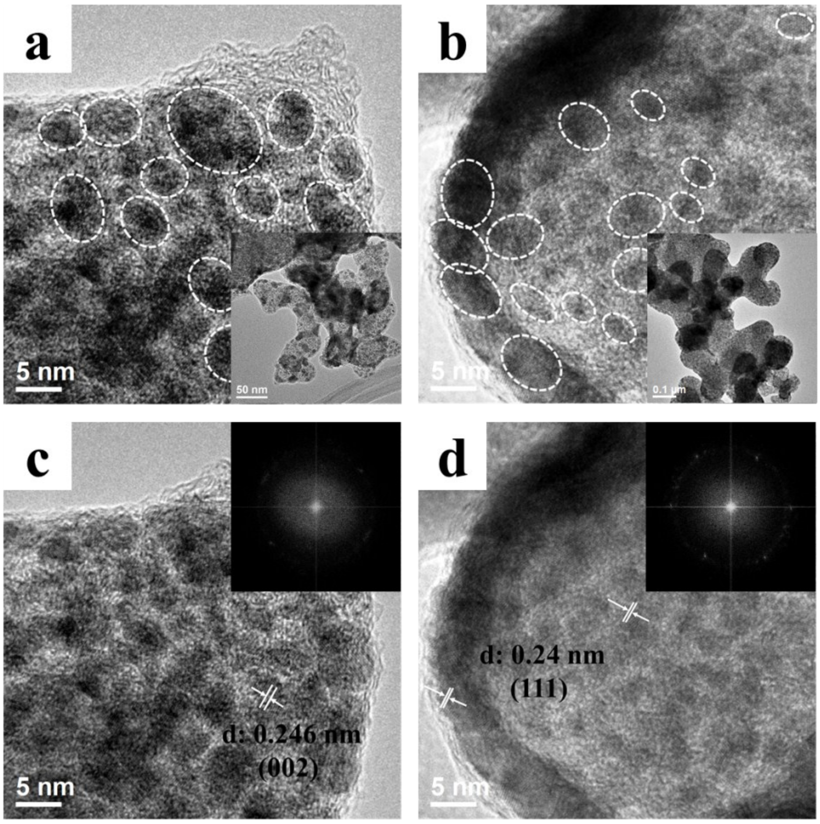

Figure S5. TEM images of o-α-Mo_2C@BCN (**a**), c-α-MoC_{1-x}@BCN (**b**), o-α-Mo_2C@BCN (**c**) and c-α-MoC_{1-x}@BCN (**d**). Insets are low magnification (**a,b**) and Forward Fourier Transform (FFT) images.

a

b

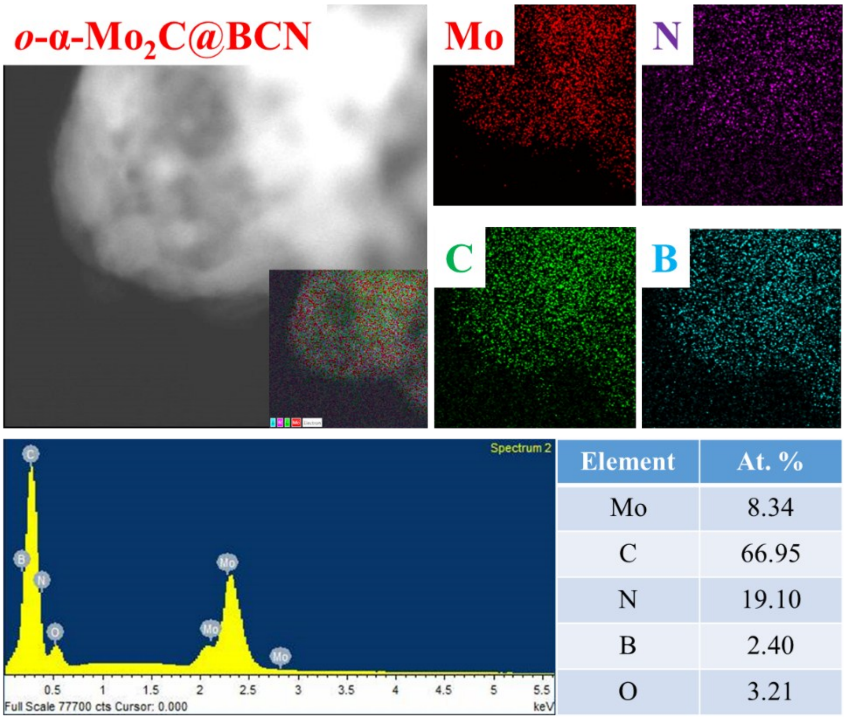

Element	At. %
Mo	8.34
C	66.95
N	19.10
B	2.40
O	3.21

Figure S6. EDX elemental mapping of (a) o-α-Mo_2C@BCN (inset combined image of elemental mapping) and (b) EDS-SEM spectrum with composition in Table.

a

b

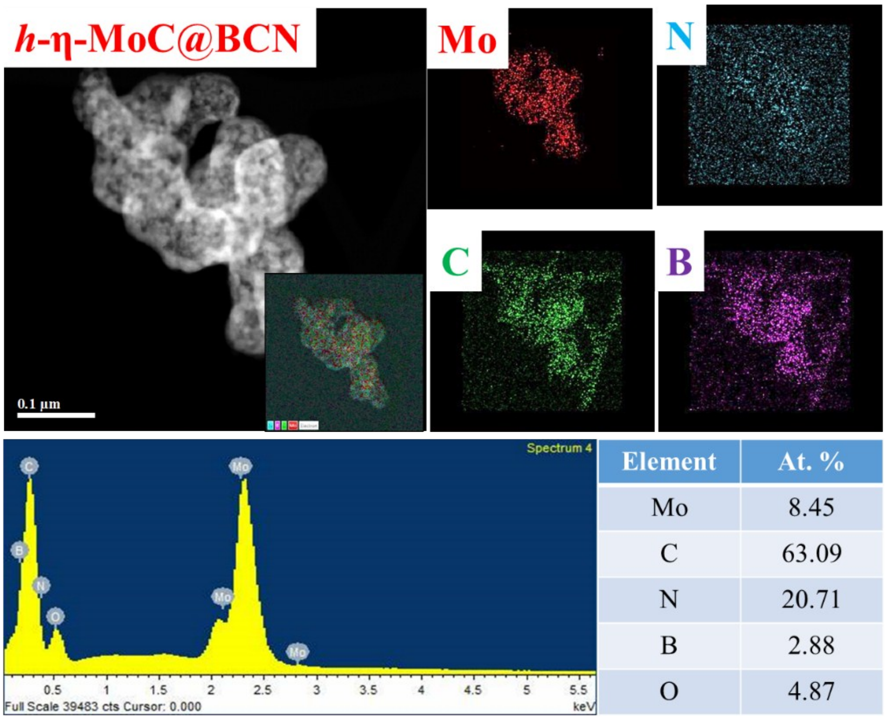

Element	At. %
Mo	8.45
C	63.09
N	20.71
B	2.88
O	4.87

Figure S7. EDX elemental mapping of (a) h-η-MoC@BCN (inset combined image of elemental mapping) and (b) EDS-SEM spectrum with composition in Table.

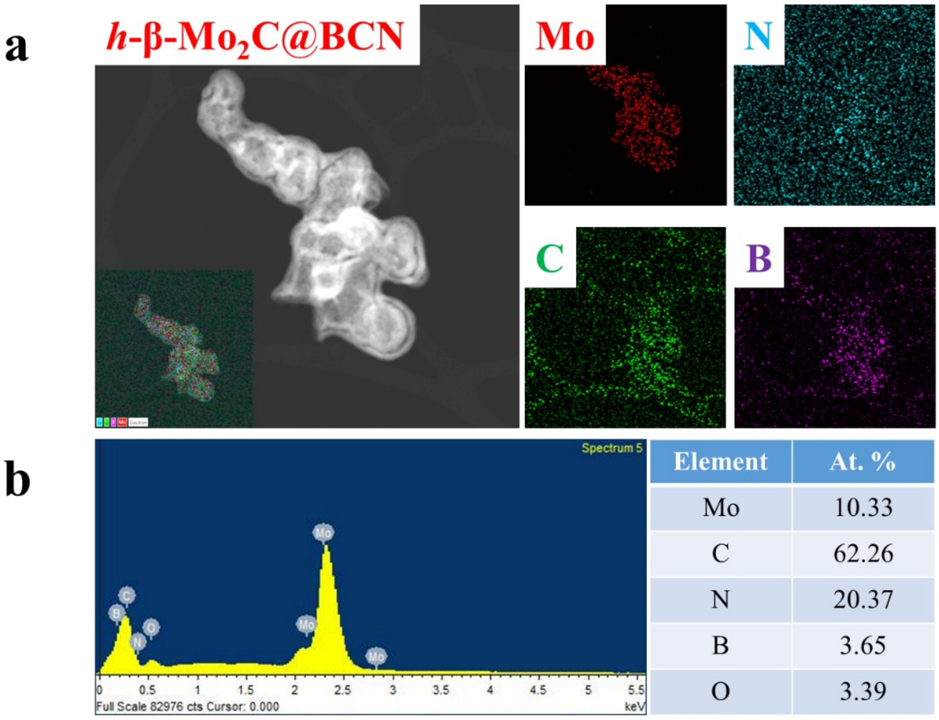

Element	At. %
Mo	10.33
C	62.26
N	20.37
B	3.65
O	3.39

Figure S8. EDX elemental mapping of (a) h-β-Mo_2C@BCN (inset combined image of elemental mapping) and (b) EDS-SEM spectrum with composition in Table.

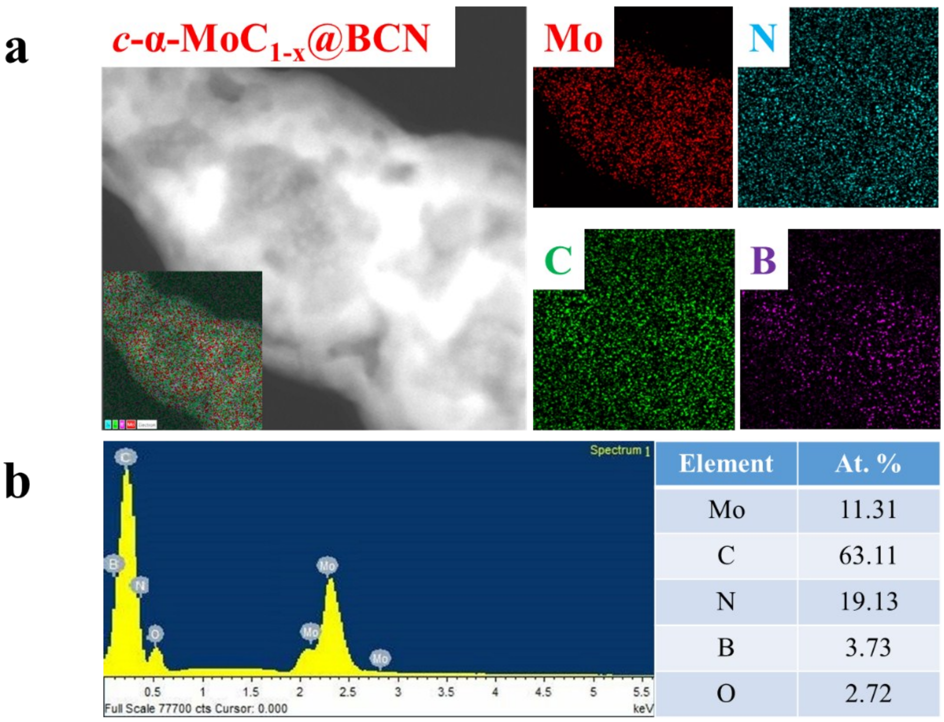

Element	At. %
Mo	11.31
C	63.11
N	19.13
B	3.73
O	2.72

Figure S9. EDX elemental mapping of (a) c-α-MoC_{1-x}@BCN (inset combined image of elemental mapping) and (b) EDS-SEM spectrum with composition in Table.

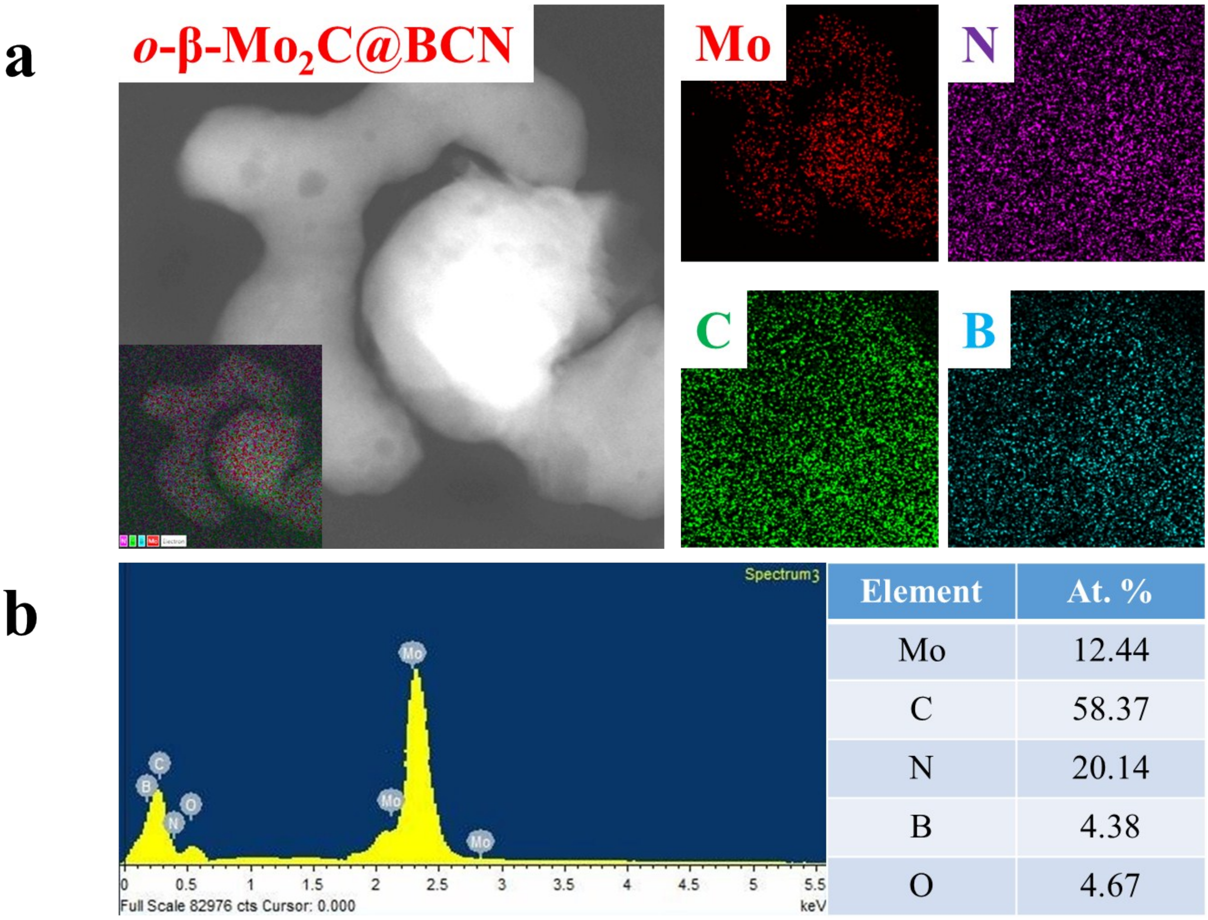

Element	At. %
Mo	12.44
C	58.37
N	20.14
B	4.38
O	4.67

Figure S10. EDX elemental mapping of (a) o-β-Mo_2C@BCN (inset combined image of elemental mapping) and (b) EDS-SEM spectrum with composition in Table.

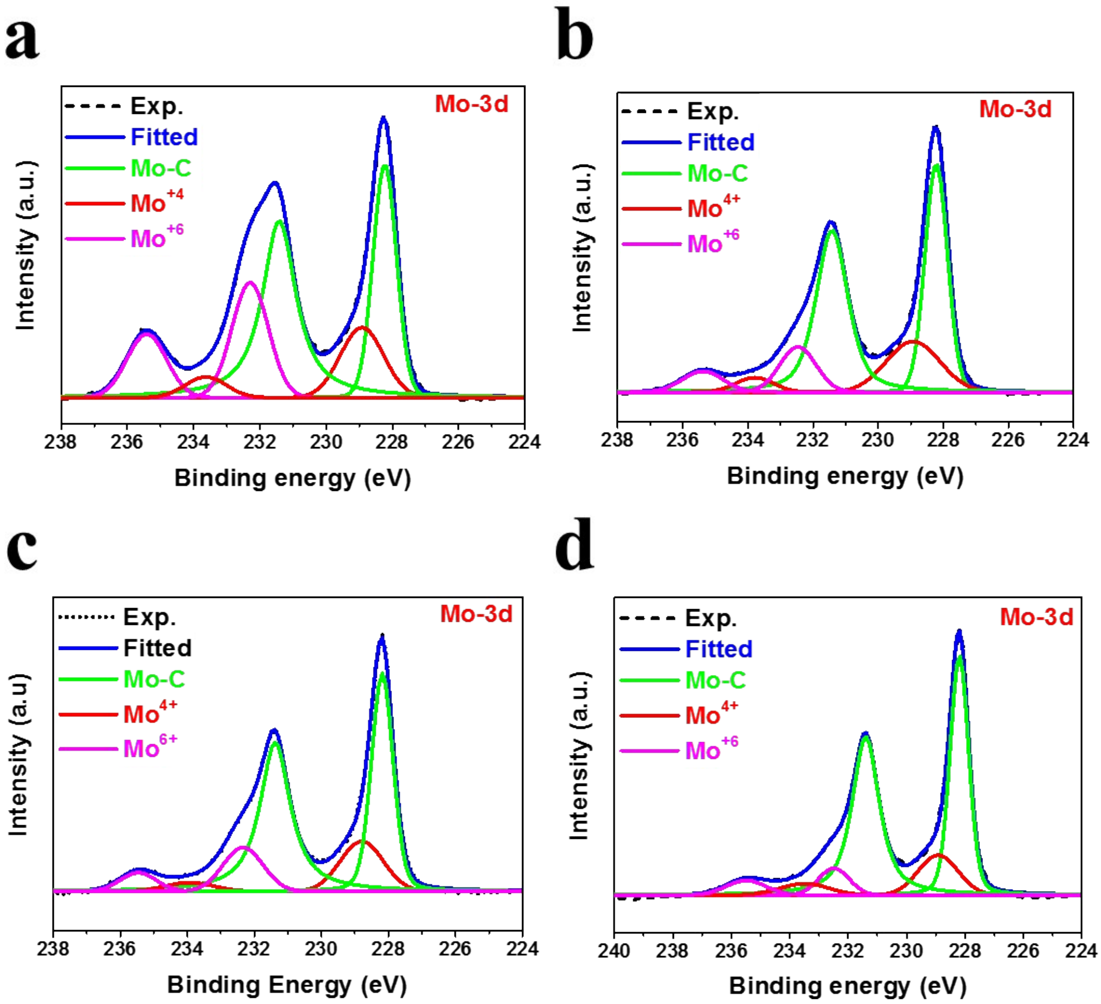

Figure S11. X-ray photoelectron spectroscopy (XPS) spectra: a) Orthorhombic α-Mo_2C@BCN; b) Hexagonal η-MoC@BCN; c) Hexagonal β-Mo_2C@BCN; d) Orthorhombic β-Mo_2C@BCN.

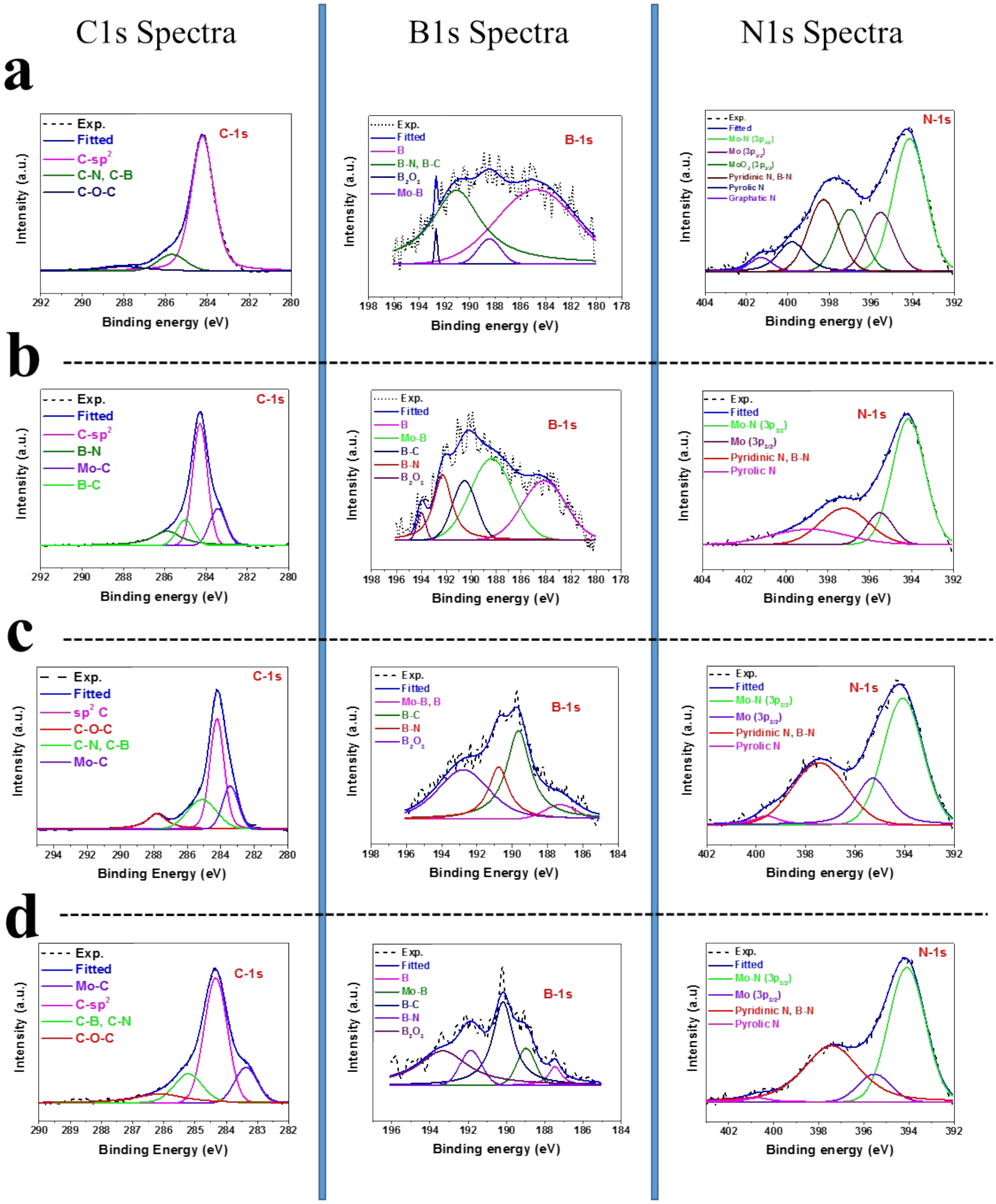

Figure S12. XPS spectra (without background) and fitted peaks of C1s, B1s and N1s for (a) orthorhombic α-Mo_2C@BCN, (b) hexagonal η-MoC@BCN, (c) hexagonal β-Mo_2C@BCN, and (d) orthorhombic β-Mo_2C@BCN

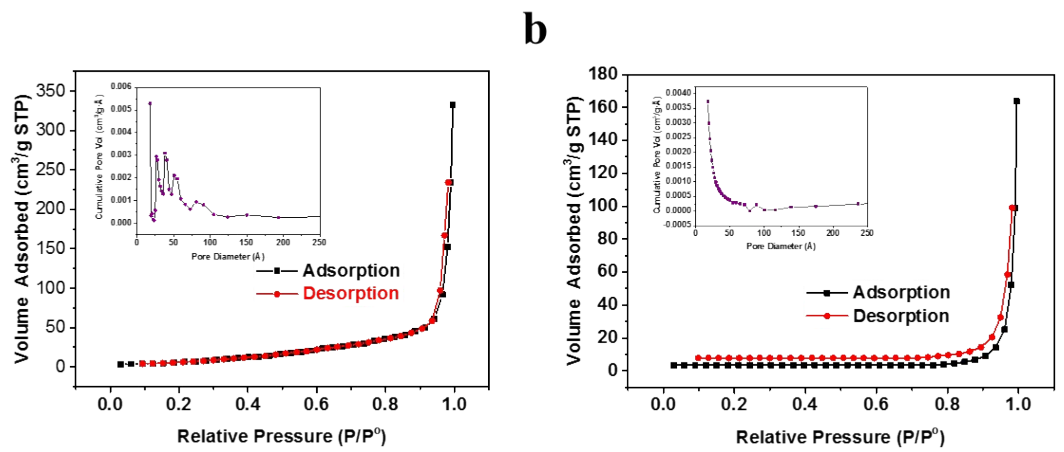

Figure S13. Nitrogen adsorption-desorption isotherms of (**a**) hexagonal β-Mo_2C@BCN and (**b**) cubic α-MoC_{1-x}@BCN. Insets show pore size distributions.

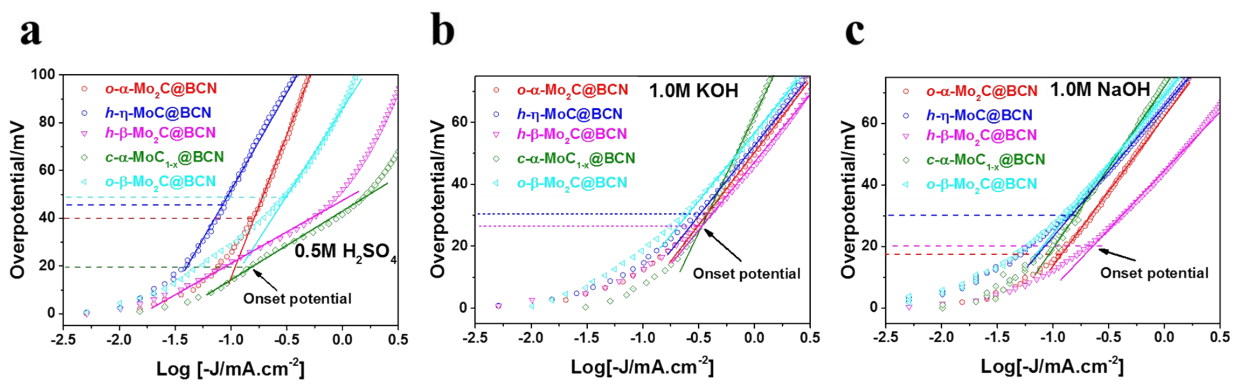

Figure S14. Tafel plots in of low current densities region of all hybrid electrocatalysts in 0.5M H_2SO_4 (**a**), 1.0M KOH (**b**) and 1.0M NaOH (**c**). The onset overvoltage is determined by the potential when the Tafel plots begin to deviate from the linear region as indicated by the arrow.

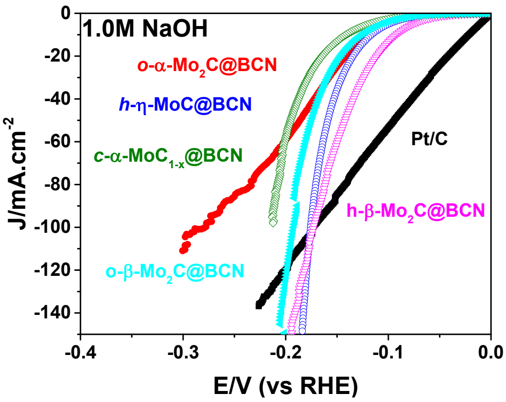

Figure S15. Out-class HER performance of hybrid catalysts than Pt/C at higher current densities in alkaline media

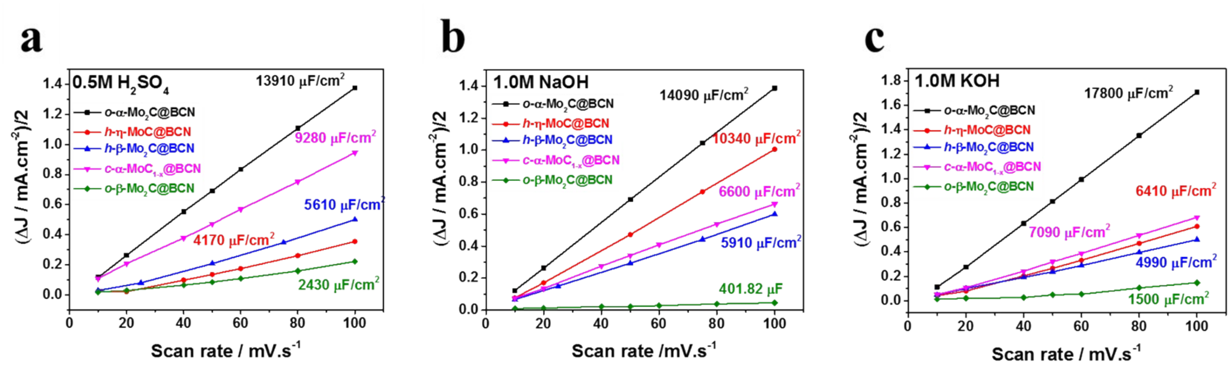

Figure S16. Half of current density differences ($\Delta j= J_a-J_c$) plotted against scan rates in (**a**) 0.5M H_2SO_4, (**b**) 1.0M NaOH and (**c**) 1.0M KOH. Specific capacitances (μf cm^{-2}) are equivalent to the linear slopes of each curve which is used to calculate ECSA

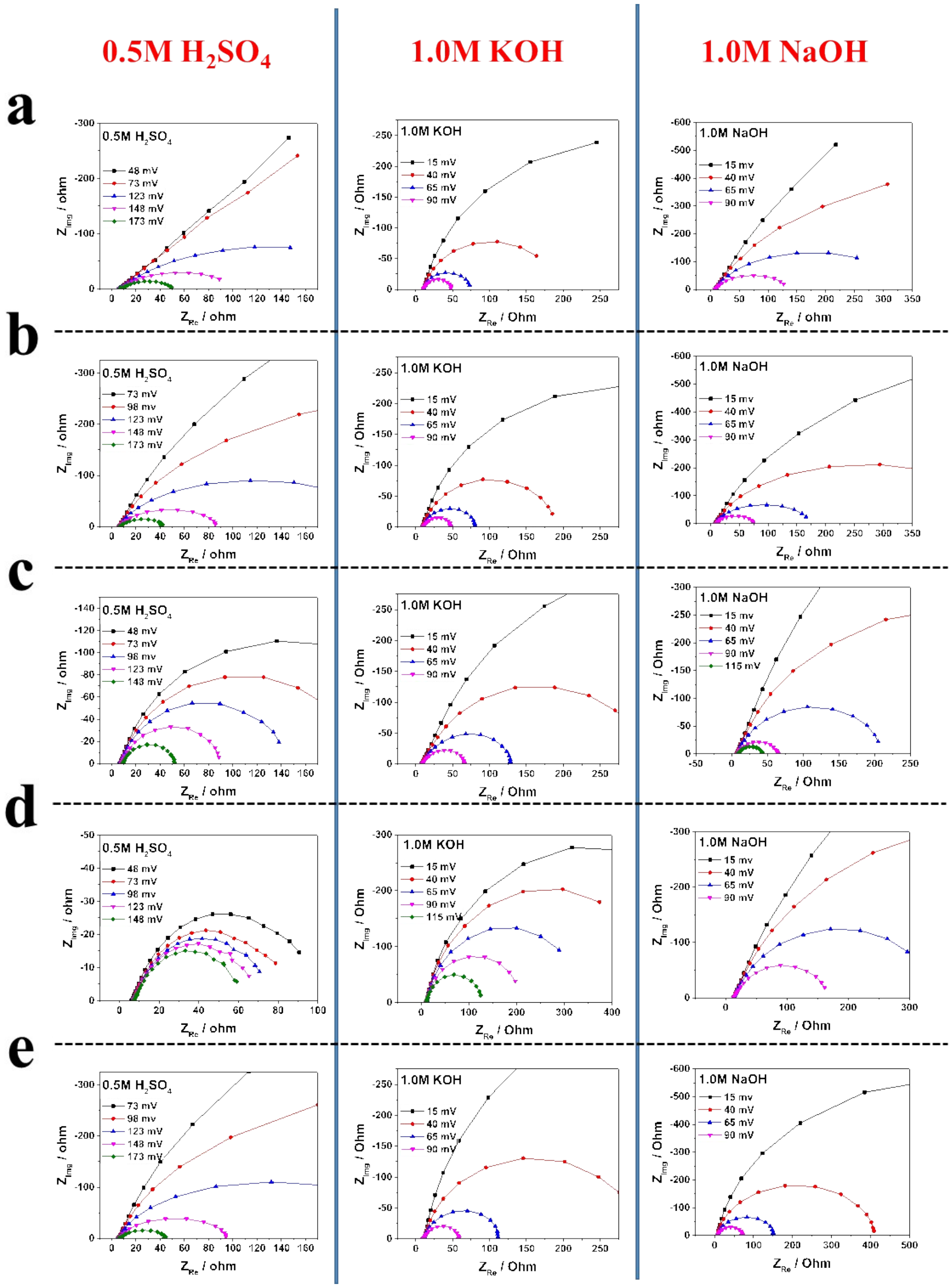

Figure S17. Electrochemical impedance spectroscopy (EIS) analysis for all composites: (**a**) for o-α-Mo_2C@BCN, (**b**) h-η-Mo_2C@BCN, (**c**) h-β-Mo_2C@BCN, (**d**) c-α-MoC_{1-x}@BCN and (**e**) o-β-Mo_2C@BCN in 0.5M H_2SO_4, 1.0M KOH and 1.0M NaOH, respectively

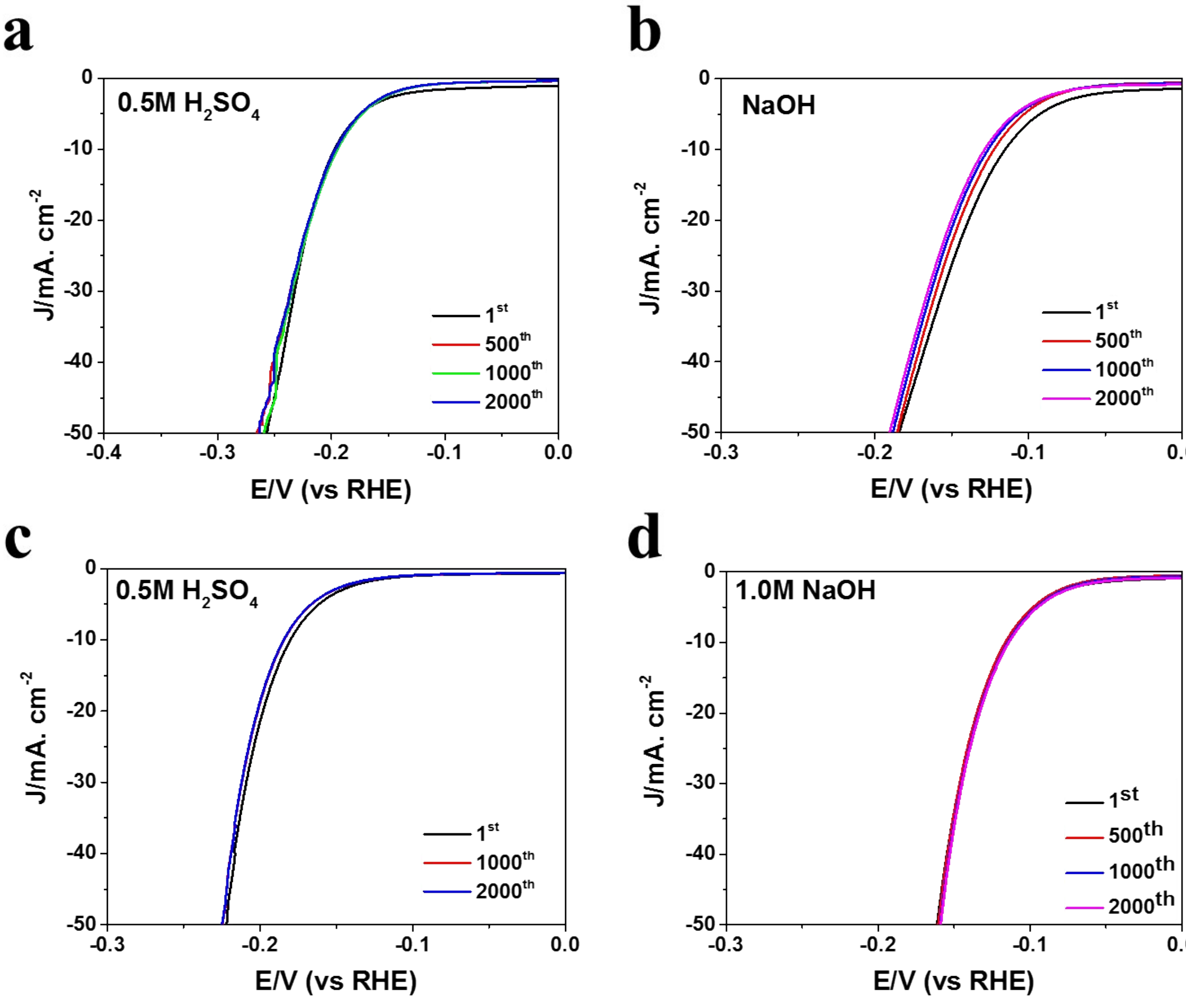

Figure S18. Polarization curves after continuous potential CV cycles up to 2000 of (**a-b**) o-α-Mo_2C@BCN and (**c-d**) h-η-Mo_2C@BCN in acidic and alkaline solutions, respectively.

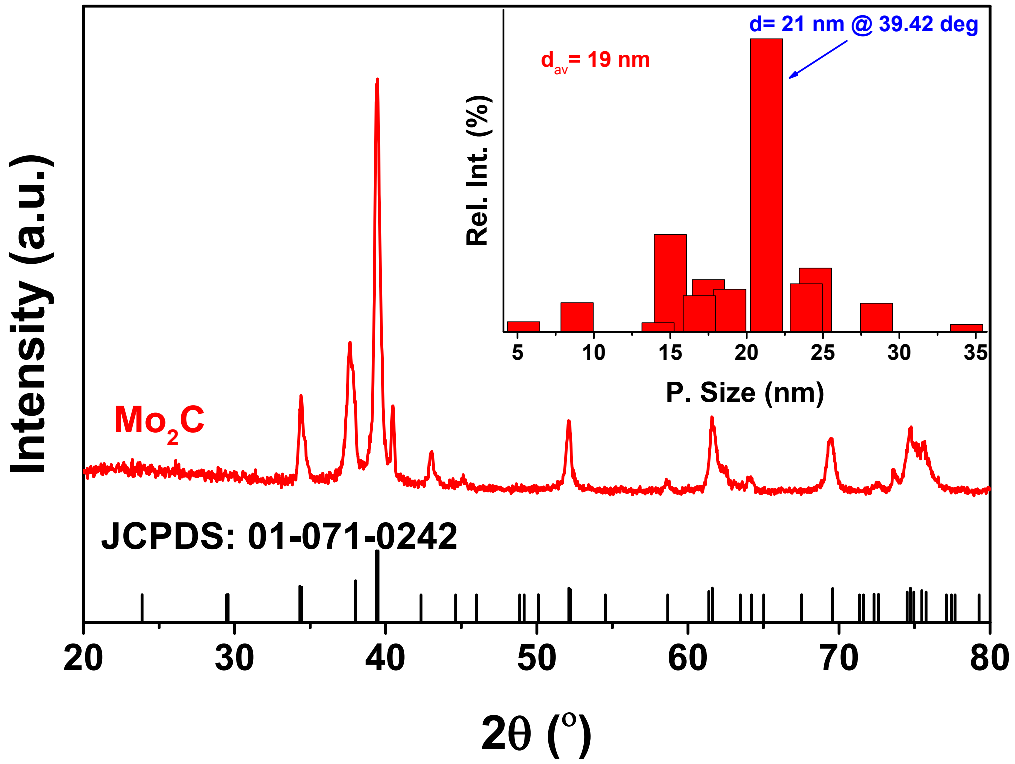

Figure S19. XRD pattern of N-doped Molybdenum carbide without BCN network, particle size distribution (inset)

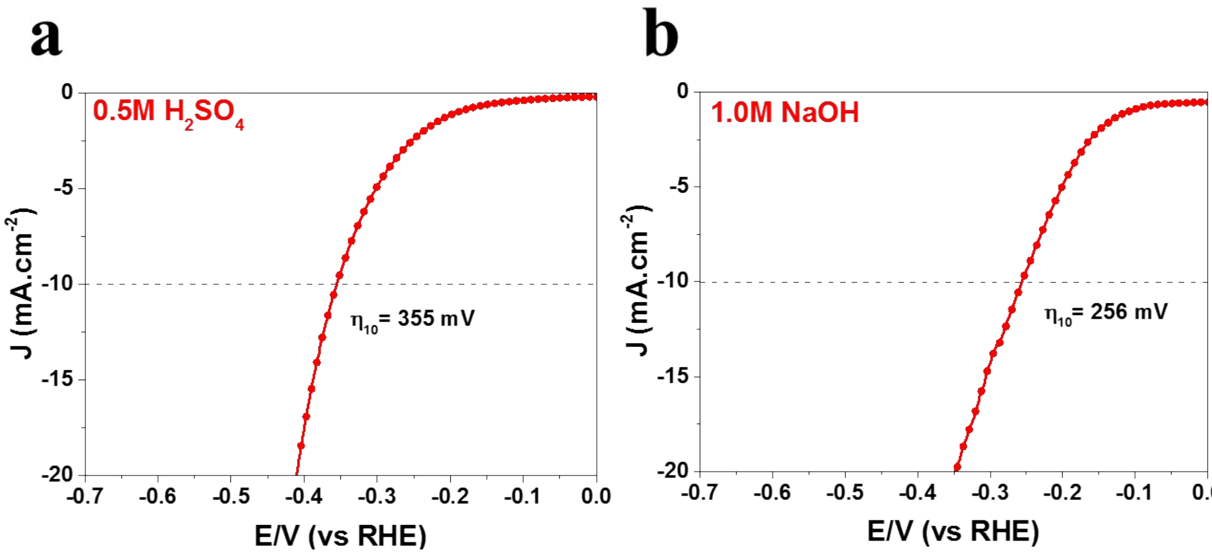

Figure S20. HER activity of N-doped molybdenum carbide without BCN protection in acidic and basic media. (**a**) 0.5M H_2SO_4 and (**b**) 1.0M NaOH

References

1 N. S. Alhajri, D. H. Anjum and K. Takanabe, *J. Mater. Chem. A*, 2014, **2**, 10548-10556.
2 S. T. Hunt, T. Nimmanwudipong and Y. Román-Leshkov, *Angew. Chem. Int. Ed.*, 2014, **53**, 5131-5136.
3 W. Cui, N. Cheng, Q. Liu, C. Ge, A. M. Asiri and X. Sun, *ACS Catal.*, 2014, **4**, 2658-2661.
4 M. Boride, *Angew. Chem. Int. Ed.*, 2012, **51**, 12703-12706.
5 C. Ge, P. Jiang, W. Cui, Z. Pu, Z. Xing, A. M. Asiri, A. Y. Obaid, X. Sun and J. Tian, *Electrochim. Acta*, 2014, **134**, 182-186.
6 L. Ma, L. R. L. Ting, V. Molinari, C. Giordano and B. S. Yeo, *J. Mater. Chem. A*, 2015, **3**, 8361-8368.
7 K. Zhang, Y. Zhao, S. Zhang, H. Yu, Y. Chen, P. Gao and C. Zhu, *J. Mater. Chem. A*, 2014, **2**, 18715-18719.
8 W.-F. Chen, S. Iyer, S. Iyer, K. Sasaki, C.-H. Wang, Y. Zhu, J. T. Muckerman and E. Fujita, *Energy Environ. Sci.*, 2013, **6**, 1818-1826.
9 C. Tang, W. Wang, A. Sun, C. Qi, D. Zhang, Z. Wu and D. Wang, *ACS Catal.*, 2015, **5**, 6956-6963.
10 W.-F. Chen, C.-H. Wang, K. Sasaki, N. Marinkovic, W. Xu, J. Muckerman, Y. Zhu and R. Adzic, *Energy Environ. Sci.*, 2013, **6**, 943-951.
11 P. Xiao, Y. Yan, X. Ge, Z. Liu, J.-Y. Wang and X. Wang, *Appl. Catal. B: Environ.*, 2014, **154**, 232-237.
12 J. Zhang, X. Meng, J. Zhao and Z. Zhu, *ChemCatChem*, 2014, **6**, 2059-2064.
13 K. Zhang, Y. Zhao, D. Fu and Y. Chen, *J. Mater. Chem. A*, 2015, **3**, 5783-5788.
14 Y. Zhao, K. Kamiya, K. Hashimoto and S. Nakanishi, *J. Am. Chem. Soc.*, 2014, **137**, 110-113.
15 H. B. Wu, B. Y. Xia, L. Yu, X.-Y. Yu and X. W. D. Lou, *Nat. Commun.*, 2015, **6**.
16 D. H. Youn, S. Han, J. Y. Kim, J. Y. Kim, H. Park, S. H. Choi and J. S. Lee, *ACS Nano*, 2014, **8**, 5164-5173.
17 L. F. Pan, Y. H. Li, S. Yang, P. F. Liu, M. Q. Yu and H. G. Yang, *Chem. Commun.*, 2014, **50**, 13135-13137.
18 L. Liao, S. Wang, J. Xiao, X. Bian, Y. Zhang, M. D. Scanlon, X. Hu, Y. Tang, B. Liu and H. H. Girault, *Energy. Environ. Sci.*, 2014, **7**, 387-392.
19 Y. Liu, G. Yu, G. D. Li, Y. Sun, T. Asefa, W. Chen and X. Zou, *Angew. Chem. Int. Ed.*, 2015, **54**, 10752-10757.
20 H. Ang, H. T. Tan, Z. M. Luo, Y. Zhang, Y. Y. Guo, G. Guo, H. Zhang and Q. Yan, *Small*, 2015, **11**, 6278-6284.
21 S. Wang, J. Wang, M. Zhu, X. Bao, B. Xiao, D. Su, H. Li and Y. Wang, *J. Am. Chem. Soc.*, 2015, **137**, 15753-15759.
22 C. Wan, Y. N. Regmi and B. M. Leonard, *Angew. Chem.*, 2014, **126**, 6525-6528.
23 H. Zhang, Z. Ma, J. Duan, H. Liu, G. Liu, T. Wang, K. Chang, M. Li, L. Shi and X. Meng, *ACS Nano*, 2015.
24 H. Vrubel and X. Hu, *Angew. Chem.*, 2012, **124**, 12875-12878.
25 J. Kibsgaard and T. F. Jaramillo, *Angew. Chem. Int. Ed.*, 2014, **53**, 14433-14437.